Journal of the Korean Electrochemical Society
Vol. 6, No. 2, 2003, 119-129

The Phase-Shift Method for the Langmuir Adsorption Isotherms at the Noble Metal (Au, Rh) Electrode Interfaces

Jang H. Chun†, Sang K. Jeon, and Jae H. Lee

Department of Electronic Engineering, Kwangwoon University, Seoul 139-701, Korea

(Received November 28, 2002 : Accepted December 20, 2002)

Abstract. The Langmuir adsorption isotherms of the over-potentially deposited hydrogen (OPD H) for the cathodic H_2 evolution reaction (HER) at the poly-Au and Rh|0.5 *M* H_2SO_4 aqueous electrolyte interfaces have been studied using cyclic voltammetric and ac impedance techniques. The behavior of the phase shift ($0^o \leq -\phi \leq 90^o$) for the optimum intermediate frequency corresponds well to that of the fractional surface coverage ($1 \geq \theta \geq 0$) at the interfaces. The phase-shift profile ($-\phi$ vs. *E*) for the optimum intermediate frequency, i.e., the phase-shift method, can be used as a new electrochemical method to determine the Langmuir adsorption isotherm (θ vs. *E*) of the OPD H for the cathodic HER at the interfaces. At the poly-Au|0.5 *M* H_2SO_4 aqueous electrolyte interface, the equilibrium constant (*K*) and the standard free energy (ΔG_{ads}) of the OPD H are 2.3×10^{-6} and 32.2 kJ/mol, respectively. At the poly-Rh|0.5 *M* H_2SO_4 aqueous electrolyte interface, *K* and ΔG_{ads} of the OPD H are 4.1×10^{-4} or 1.2×10^{-2} and 19.3 or 11.0 kJ/mol depending on *E*, respectively. In contrast to the poly-Au electrode interface, the two different Langmuir adsorption isotherms of the OPD H are observed at the poly-Rh electrode interface. The two different Langmuir adsorption isotherms of the OPD H correspond to the two different adsorption sites of the OPD H on the poly-Rh electrode surface.

Key words : Phase-shift method; Langmuir adsorption isotherm; Over-potentially deposited hydrogen; Au and Rh electrodes

1. Introduction

The cathodic hydrogen evolution reaction (HER) at noble and transition metal (Pt, Ir, Rh, Pd, Au, Ni)|aqueous electrolyte interfaces is one of the most extensively studied interfacial electrochemistry. Many electrochemical methods, e.g., cyclic voltammetric and electrochemical impedance spectroscopic methods, have been used to study the adsorption processes of the under-potentially deposited hydrogen (UPD H) and the over-potentially deposited hydrogen (OPD H) for the cathodic HER at the interfaces[1-4]. However, the kinetics and mechanisms of the cathodic HER have been studied mainly using steady state polarization experiments and so there are quite few reliable kinetic data, i.e., the equilibrium constant and the fractional surface coverage due to the adsorption process of the OPD H, at the interfaces. In addition, the phase-shift method, i.e., the relationship between the phase-shift profile for the optimum intermediate frequency and the Langmuir or the Frumkin adsorption isotherm, has not been developed or suggested to study the adsorption processes of the UPD H and the OPD H for the cathodic HER at the interfaces.

The relation, transition, and criterion of the UPD H and the OPD H have been studied to understand the kinetics and mechanisms of the cathodic HER at the noble metal (Pt, Ir, Rh, Pd, Au)|aqueous electrolyte interfaces[6-15]. It is well known that the UPD H and the OPD H occupy different surface adsorption sites and act as two distinguishable electroadsorbed H species while only the OPD H can contribute to the cathodic HER. However, the relation, transition, and criterion of the UPD H and the OPD H at the interfaces have been studied on a point of view of the H_2 evolutions and potentials rather than the H adsorption sites and processes, i.e., the Langmuir or the Frumkin adsorption isotherms.

The Langmuir adsorption isotherm is based on the kinetics and thermodynamics of the electrode interfaces. Although the Langmuir adsorption isotherm may be regarded a classical model and theory in physical electrochemistry[16], it is useful and effective to study the H adsorption sites and processes for the cathodic HER at the interfaces. Thus, there is a need in the art for a fast, simple, and reliable technique to estimate or determine the Langmuir adsorption isotherms for characterizing the relation, transition, and criterion between the UPD H and the OPD H for the cathodic HER at the interfaces.

Recently, we have experimentally and consistently found that the phase-shift method can be effectively used to estimate the Langmuir or the Frumkin adsorption isotherms of the UPD H and the OPD H for the cathodic HER at noble and transition metal (Pt, Ir, Pd, Pt-Rh, Au, Rh, Ni)|aqueous electrolyte interfaces[17-24]. It is useful and effective for studying the electrode kinetics and the relation, transition, and criterion between the UPD H and the OPD H for the cathodic HER at the interfaces.

In this paper we will represent the Langmuir adsorption isotherms of the OPD H for the cathodic HER at the poly-Au

†E-mail: jhchun@daisy.kwangwoon.ac.kr

and Rh|0.5 M H_2SO_4 aqueous electrolyte interfaces using the phase-shift method. Partially, it is complementary to the Langmuir adsorption isotherm of the OPD H for the cathodic HER at the poly-Au electrode interface[22]. It appears that the phase-shift method is useful and effective to study the electrode kinetics and thermodynamics of the OPD H for the cathodic HER at the poly-Au and Rh electrode interfaces.

2. Experimental

2.1. Preparations

Taking into account H^+ concentrations and effects of diffuse double layer and pH[25], an acidic aqueous electrolyte was prepared from H_2SO_4 (Junsei, special grade) with purified water (resistivity: >18 MΩ cm) obtained from a Millipore system. The 0.5 *M* H_2SO_4 aqueous electrolyte was deaerated with 99.999% purified nitrogen gas for 20 min before the experiments.

A standard 3-electrode configuration was employed using an SCE reference electrode and a poly-Au wire (Johnson Matthey, purity: 99.999%, 1 mm diameter, estimated surface area: ~0.57 cm^2) or a poly-Rh wire (Johnson Matthey, purity: 99.8%, 1 mm diameter, estimated surface area: ~1.17 cm^2) working electrode. Both the poly-Au and Rh working electrodes were prepared by flame cleaning and then quenched and cooled in the Millipore Milli-Q water and in air, sequentially. A Pt wire (Johnson Matthey, purity: 99.95%, 1.5 mm diameter) was used as a counter electrode. Taking into account the OPD H and its current distribution[26], the working and counter electrodes were separately placed (~4 cm) in the same compartment Pyrex cell using Teflon holders.

2.2. Measurements

Cyclic voltammetric (scan potential: -0.30 to 1.65 V vs. SCE, scan rate: 200 mV/s) and ac impedance (single sine wave, scan frequency: 10^4 to 1 Hz, ac amplitude: 5 mV, dc potential: 0 to -0.575 V vs. SCE) techniques were used to study the relation between the phase-shift profile for the optimum intermediate frequency and the corresponding Langmuir adsorption isotherm. The high scan rate (>100 mV/s) was used to measure the state of the poly-Au and Rh working electrodes at the commencement of the cyclic scan[26].

The cyclic voltammetric experiment was performed using an EG&G PAR Model 273A potentiostat controlled with the PAR Model 270 software package. The ac impedance experiment was performed using the same apparatus in conjunction with a Schlumberger SI 1255 HF Frequency Response Analyzer controlled with the PAR Model 388 software package. In order to obtain comparable and reproducible results, all measurements were carried out using the same preparations, procedures, and conditions at room temperature. The international sign convention is used, i.e., cathodic currents and lagged phase shifts or angles are taken as negative. Finally, in order to clarify the hydrogen adsorption in the different aqueous electrolytes, all potentials in the text, the Figures, and the Tables are given on the RHE (Reversible Hydrogen Electrode) scale.

3. Results and Discussion

3.1. UPD H peak

Figure 1 shows the typical cyclic voltammogram of the steady state at the poly-Au|0.5 *M* H_2SO_4 aqueous electrolyte interface. As pointed out by Jerkiewicz *et al.*[14,15], the UPD H peak is not experimentally observable at the interface. Since, the under-potentially deposited oxygen atoms are formed on the adsorption sites of the UPD H and so the plateau occurs at ca. 0.141 to -0.079 V vs. RHE. The plateau corresponds to the total charge passed during ionization of the under-potentially deposited oxygen atoms on the adsorption sites of the UPD H. However, it implies that the Langmuir adsorption isotherm of the UPD H cannot be obtained at the cathodic potential range. Consequently, it can be interpreted that the cathodic HER on the poly-Au electrode surface seems to occur only on the adsorption sites of the OPD H. The anionic adsorption effects, which are not serious for the adsorption process of the OPD H, on the adsorption sites of the UPD H have not been considered[1,13]. The UPD H peak and the corresponding cathode potential are necessary and useful to verify the Langmuir adsorption isotherm of the UPD H or the OPD H for the cathodic HER at the interface.

3.2. Phase-shift profile for the optimum intermediate frequency

The equivalent circuit for the cathodic HER is usually expressed as shown in Fig. 2(a)[27-29]. Taking into account the relaxation time effect, which is inevitable under the ac impedance experiment[6,30], the equivalent circuit elements shown in Fig. 2(a) are defined as: R_S is the electrolyte resistance, R_F is the equivalent resistance due to the adsorption process of H, i.e., the UPD H and/or the OPD H, and its relaxation time effect at the interface, R_P is the equivalent resistance due to the recombination reaction, C_P is the equivalent capacitance due to the adsorption process of H, i.e., the UPD H and/or the OPD H, and its relaxation time effect at the interface, and C_D is the double-layer capacitance. The impedance (Z)

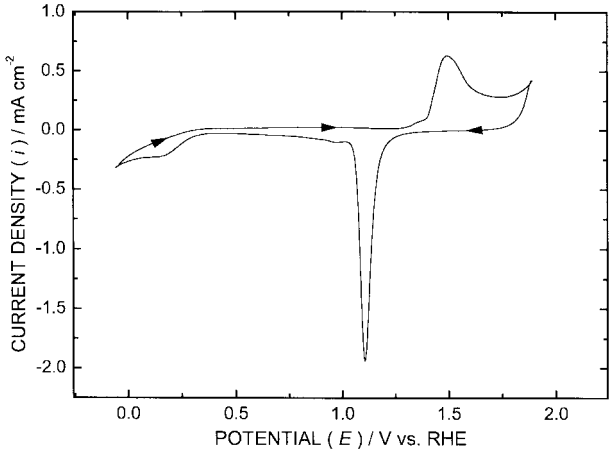

Fig. 1. The typical cyclic voltammogram at the poly-Au|0.5 *M* H_2SO_4 aqueous electrolyte interface. Estimated surface area: ~0.57 cm^2. Scan potential: -0.059 to 1.891 V vs. RHE. Scan rate: 200 mV/s. 10th scan.

of the equivalent circuit shown in Fig. 2(a) is given by:

$$Z = R_S + \{(R_F + R_P + j\omega R_F R_P C_P)/[1 - \omega^2 R_F R_P C_P C_D + j\omega(R_P C_P + R_F C_D + R_P C_D)]\} \quad (1)$$

where j is an operator and is equal to the square root of -1, i.e., $j^2 = -1$, and ω (= $2\pi f$) is the angular frequency.

The two equivalent circuit elements, i.e., R_F and C_P, are the equivalent resistance and capacitance associated with the faradaic resistance (R_ϕ) and the adsorption pseudocapacitance (C_ϕ) of the UPD H and/or the OPD H, respectively. Under the ac impedance experiment, R_F is smaller than R_ϕ due to the relaxation times of the previously adsorbed H, i.e., the increase of H^+ on the electrode surface. On the other hand, C_P is greater than C_ϕ due to the relaxation times of the previously adsorbed H, i.e., the increase of H^+ on the electrode surface. Since, in general, a resistance is inversely proportional to charged species but a capacitance is proportional to charged species. It implies that the relaxation time effects of R_F and C_P can be cancelled out or compensated together.

Essentially, both the relaxation time and lateral interaction effects at the interface are proportional to the fractional surface coverage of the UPD H and/or the OPD H. It implies that the behavior of R_F and C_P depends strongly on that of R_ϕ and C_ϕ. Also, it implies that the lateral interaction effect depends strongly on R_F and C_P, i.e., R_ϕ and C_ϕ. Therefore, the adsorption process of the UPD H and/or the OPD H corresponding to the combination of R_F and C_P can be correctly expressed in terms of the phase delay. This aspect was not well interpreted in the previously published papers[17,18]. Of course, the experimental results presented there and related discussions are unchanged. However, it is well known that the fractional surface coverage depends on the applied dc potential at the interface. Also, it is well known that the phase shift or angle depends on the applied dc potential at the interface.

The frequency responses of the equivalent circuit shown in Fig. 2(a) are important and useful to study the relationship between the phase shift and the fractional surface coverage for the cathodic HER at the interface. At low frequencies, the equivalent circuit can be expressed as a series circuit of R_S, R_F, and R_P. At high frequencies, the equivalent circuit can be expressed as a series circuit of R_S and C_D. At intermediate frequencies, the equivalent circuit can be simplified as a series circuit of R_S, R_F, and C_P shown in Fig. 2(b)[27,28]. In practice, R_P is much greater than R_F. Also, C_P is much greater than C_D except at $\theta \approx 0$. In addition, R_P is much greater than $|1/\omega C_P|$ for the intermediate frequencies. Therefore, R_P and C_D can be eliminated from the equivalent circuit for the cathodic HER shown in Fig. 2(a). It implies that the simplified equivalent circuit for the intermediate frequencies shown in Fig. 2(b) can be applied to the poly-Au and Rh|0.5 M H_2SO_4 aqueous electrolyte interfaces regardless of H_2 evolution. However, it should be noted that the simplified equivalent circuit shown in Fig. 2(b) is not change of the cathodic HER itself but only the intermediate frequency response itself. In other words, it is valid and effective for studying the UPD H and/or the OPD H at the interfaces. The frequency responses of the equivalent

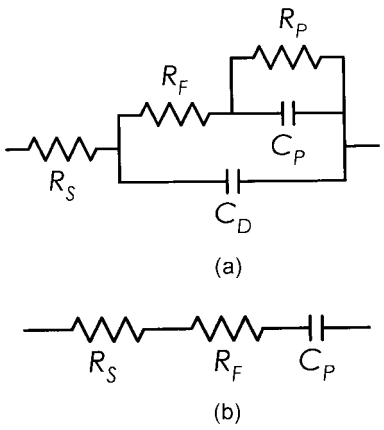

Fig. 2. (a) The equivalent circuit for the cathodic H_2 evolution reaction at the poly-Au|0.5 *M* H_2SO_4 aqueous electrolyte interface and (b) The simplified equivalent circuit for the intermediate frequencies at the interface.

circuit shown in Fig. 2(a) are described elsewhere[27].

The impedance (Z) of the equivalent circuit for the intermediate frequencies shown in Fig. 2(b) and the corresponding phase shift (ϕ) or angle are given by[31]:

$$Z = (R_S + R_F) - j/\omega C_P \quad (2)$$

$$\phi = -\tan^{-1}[1/\omega(R_S + R_F)C_P] \quad (3)$$

$$R_F \propto R_\phi\ (< R_\phi),\ R_F > R_S,\ C_P > C_D, \text{ and } C_P \propto C_\phi\ (> C_\phi) \quad (4)$$

where R_ϕ is the faradaic resistance for the discharge reaction of the UPD H or the OPD H and depends on the fractional surface coverage (θ) of the UPD H or the OPD H, and C_ϕ is the adsorption pseudocapacitance and also depends on θ[27-29,32]. It should be noted that both R_ϕ (or R_F) and C_ϕ (or C_P) cannot exist unless charge is transferred across the interphase.

A minus sign shown in Eq. 3 implies a lagged phase. In practice, the value of R_S at the poly-Au|0.5 M H_2SO_4 aqueous electrolyte interface is ~1-1.4 Ω cm^2 which can be neglected comparing to that of R_F (Fig. 3). Therefore, from Eq. 3, it is readily understood that the lagged phase depends strongly on R_F and C_P, i.e., R_ϕ and C_ϕ or θ. It was pointed out by Gileadi and Conway[32] that the shape of the C_ϕ vs. E is the exact form of the θ vs. E. It implies that the lagged phase shift ($-\phi$) also depends markedly on the adsorption process of the UPD H and/or the OPD H at the interface. However, as previously described, it should not be confused C_P with C_ϕ which has a maximum value at $\theta = 0.5$ and can be neglected at $\theta \approx 0$ and 1[27-29,32]. Also, it should not be confused that the simplified equivalent circuit shown in Fig. 2(b) is not change of the cathodic HER itself but only the intermediate frequency response itself. Consequently, it is understood that the simplified equivalent circuit for the intermediate frequencies is effective and valid to determine the Langmuir adsorption isotherm for the cathodic HER.

Figures 3(a) and (b) show the profiles of the measured R_F and C_P versus the cathode potential (E) for the optimum inter-

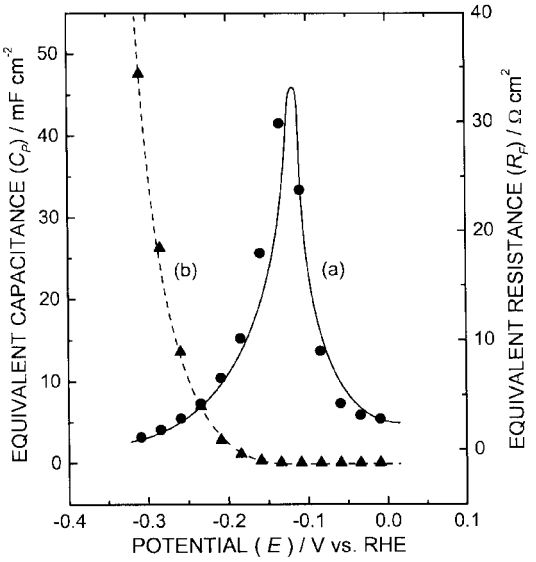

Fig. 3. The profiles of the measured equivalent circuit elements (R_P, C_P) versus E for the optimum intermediate frequency (ca. 100 Hz) at the poly-Au|0.5 M H_2SO_4 aqueous electrolyte interface. Single sine wave. Scan frequency: 10^4 to 1 Hz. ac amplitude: 5 mV. dc potential: -0.009 to -0.309 V vs. RHE. (a) Equivalent resistance profile (R_F vs. E) and (b) Equivalent capacitance profile (C_P vs. E).

mediate frequency (ca. 100 Hz) at the poly-Au|0.5 M H_2SO_4 aqueous electrolyte interface, respectively. As previously described, Fig. 3(a) shows that R_F is smaller than R_ϕ. Since, the left-hand side of the profile (R_F vs. E) is lower than the right-hand side of the profile. It is attributed to the superposition of the Langmuir adsorption process and the relaxation time effect, and the nature of resistance which is inversely proportional to charged species. On the other hand, as previously described, Fig. 3(b) shows that C_P is greater than C_ϕ. Since, the profile (C_P vs. E) increases from the right-hand side to the left-hand side, i.e., towards more negative potentials. Similarly, it is attributed to the superposition of the Langmuir adsorption process and the relaxation time effect, and the nature of capacitance which is proportional to charged species. However, it should be noted that the equivalent resistance profile (R_F vs. E) shown in Fig. 3(a) has the peak due to the Langmuir adsorption process. On the other hand, the equivalent capacitance profile (C_P vs. E) shown in Fig. 3(b) has not the peak due to the relaxation time effect. It implies that the H^+ at the interface increases consistently with increase of the applied dc potential, i.e., the cathode potential, or the fractional surface coverage. As previously described, it is attributed to the superposition of the Langmuir adsorption process and the relaxation time effect, and the reciprocal nature between the resistance and the capacitance at the interface. It also implies that the relaxation time effects of R_F and C_P depend strongly on θ. However, it should be noted that Fig. 3(b) shows that C_P increases rapidly beyond the peak potential (ca. -0.129 V vs. RHE) of the equivalent resistance profile (R_F vs. E). It is understood that C_ϕ has a maximum value at the peak potential, i.e., $\theta = 0.5$, due to the Langmuir adsorption process. The determination of the optimum intermediate frequency is discussed in more detail later. Consequently, it can be interpreted that the relaxation time effects of R_F and C_P are the useful and unique feature to analyze the adsorption process of H at the poly-Au|0.5 M H_2SO_4 aqueous electrolyte interface. The relaxation time effects of R_F and C_P are essentially cancelled out or compensated together. The lateral interaction effect of the Langmuir adsorption process is negligible at the interface.

From Figs. 2(b), 3, and Eq. 3, it is understood that the real surface area problem of the poly-Au electrode is not important or serious to study the phase-shift profile. Since, the real surface area effects of R_F and C_P are completely cancelled out or compensated together. Also, it is understood that the adsorption process of H at the interface can be expressed in terms of the lagged phase. In practice, R_F is greater than R_S and so the lagged phase shift (-ϕ) can be substantially determined by the series circuit of R_F and C_P. In other words, -ϕ is substantially characterized by the series circuit of R_ϕ and C_ϕ or θ, i.e., the adsorption process of the UPD H and/or the OPD H. It implies that the behavior of the phase shift ($0° \leq -\phi \leq 90°$) for the optimum intermediate frequency can be related to that of the fractional surface coverage ($1 \geq \theta \geq 0$). It also implies that the change rate of $\Delta(-\phi)/\Delta E$ or $d(-\phi)/dE$ corresponds well to that of $\Delta\theta/\Delta E$ or $d\theta/dE$ (Fig. 7). This is discussed in more detail later. However, it appears that the mathematical relation between the phase shift (-ϕ) and the fractional surface coverage has not been derived or reported elsewhere.

Figure 4 shows the comparison of the two extremely distinguishable frequency responses at the poly-Au|0.5 M H_2SO_4 aqueous electrolyte interface. The absolute value of the impedance vs. the frequency ($|Z|$ vs. f) is plotted on a log-log scale. In Fig. 4(a), the slope portion of the frequency response curve represents the capacitive behavior of the poly-Au|0.5 M H_2SO_4 electrolyte interface. Since, a slope of -1 represents the ideal capacitive behavior. It implies that the

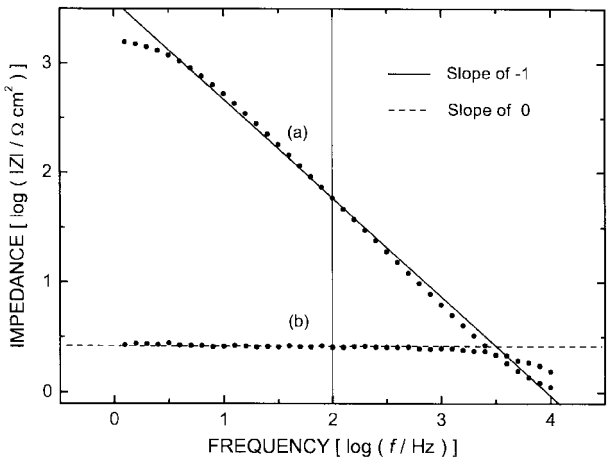

Fig. 4. The comparison of the two extremely distinguishable frequency response curves at the poly-Au|0.5 M H_2SO_4 aqueous electrolyte interface. Vertical solid line: ca. 100 Hz. Single sine wave. Scan frequency: 10^4 to 1 Hz. ac amplitude: 5 mV. dc potential: (a) -0.059 V and (b) -0.309 V vs. RHE.

Langmuir adsorption process of H and its relaxation time effect at the interface are minimized. In other words, θ can be set to zero as shown in Table 1. Therefore, from Eq. 3, -ϕ has a maximum value (≤ 90°) as shown in Fig. 5(a). On the other hand, in Fig. 4(b), the horizontal portion of the frequency response curve represents the resistive behavior of the poly-Au|0.5 M H_2SO_4 aqueous electrolyte interface. Since, a slope of zero represents the ideal resistive behavior. It implies that the Langmuir adsorption process of H and its relaxation time effect at the interface are maximized or almost saturated. In other words, θ of the OPD H can be set to unity as shown in Table 1. Therefore, from Eq. 3, -ϕ has a minimum value (≥ 0°) as shown in Fig. 5(e).

Figure 5 shows the comparison of the phase-shift curves (-ϕ vs. *f*) for the different cathode potentials at the poly-Au|0.5 *M* H_2SO_4 aqueous electrolyte interface. In Fig. 5, it should be noted that the lagged phase shifts or angles and related phase-shift curves are markedly characterized at the intermediate frequencies. The center (ca. 100 Hz) of a slope of 1 shown in Fig. 4(a), i.e., the center of the intermediate frequencies (ca. 30-300 Hz), can be set as the optimum intermediate frequency for the phase-shift profile (-ϕ vs. *E*). Of course, the exactly same shape of the phase-shift profile can also be obtained at ca. 30 and 300 Hz, i.e., the range of the intermediate frequencies. The determination of the optimum intermediate frequency for the phase-shift profile is described elsewhere[33]. Finally, the cathode potentials and the corresponding phase shifts for the optimum intermediate frequency (ca. 100 Hz) can be plotted as the phase-shift profile (-ϕ vs. *E*) shown in Fig. 6.

Table 1. The measured phase shift (-ϕ) for the optimum intermediate frequency (ca. 100 Hz) and the estimated fractional surface coverage (θ) at the poly-Au|0.5 *M* H_2SO_4 aqueous electrolyte interface

E (V vs. RHE)	-ϕ (deg)	θ [a]
-0.009	86.1	≈ 0
-0.034	86.0	0.001
-0.059	85.0	0.013
-0.084	80.4	0.067
-0.109	63.7	0.263
-0.134	33.8	0.630
-0.159	15.0	0.833
-0.184	7.4	0.923
-0.209	4.2	0.960
-0.234	2.4	0.981
-0.259	1.6	0.991
-0.284	1.1	0.996
-0.309	0.8	≈ 1

[a] Estimated using the measured phase shift (-ϕ).

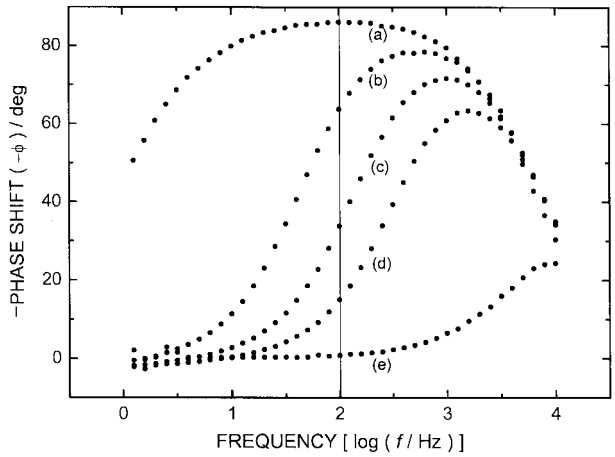

Fig. 5. The comparison of the phase-shift curves at the poly-Au|0.5 *M* H_2SO_4 aqueous electrolyte interface. Vertical solid line: ca. 100 Hz. Single sine wave. Scan frequency: 10^4 to 1 Hz. ac amplitude: 5 mV. dc potential: (a) -0.009 V, (b) -0.109 V, (c) -0.134 V, (d) -0.159 V, and (e) -0.309 V vs. RHE.

As shown in Fig. 3, the relaxation time effects of R_F and C_P are very small or negligible for the range of θ < 0.5, i.e., the right-hand side of the profile (R_F vs. *E* and C_P vs. *E*) shown in Fig. 3. It should be noted that the lateral interaction effect between the adsorbed OPD H is also negligible at the range of θ < 0.5. Therefore, the shape of the phase-shift profile (-ϕ vs. *E*) for the optimum intermediate frequency can be related to the form of the Langmuir adsorption isotherm (θ vs. *E*) at the interface. On the other hand, for the range of θ ≥ 0.5, the relaxation time effect at the interface should be considered as well as the lateral interaction effect. Since, as shown in Fig. 3, the relaxation time effects of R_F (or R_ϕ) and C_P (or C_ϕ) at the interface increase significantly with increasing of θ (≥ 0.5), i.e. beyond ca. -0.129 V vs. RHE. However, as expected, Figs. 6-8 show that the various effects and considerations, i.e., the intermediate frequency response and related equivalent circuit, the relaxation time effect, the lateral interaction effect, etc., are well supplemented and compensated together at the interface. Consequently, it can be interpreted that the form of the Langmuir adsorption isotherm (θ vs. *E*) is the exact shape of the phase-shift profile (-ϕ vs. *E*) for the optimum intermediate frequency. Both the relaxation time and lateral interaction effects on the Langmuir adsorption process are negligible at the interface.

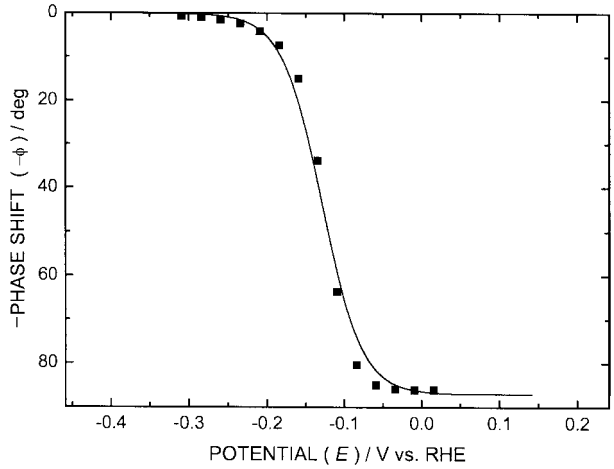

Fig. 6. The phase-shift profile (-ϕ vs. *E*) for the optimum intermediate frequency (ca. 100 Hz) at the poly-Au|0.5 *M* H_2SO_4 aqueous electrolyte interface.

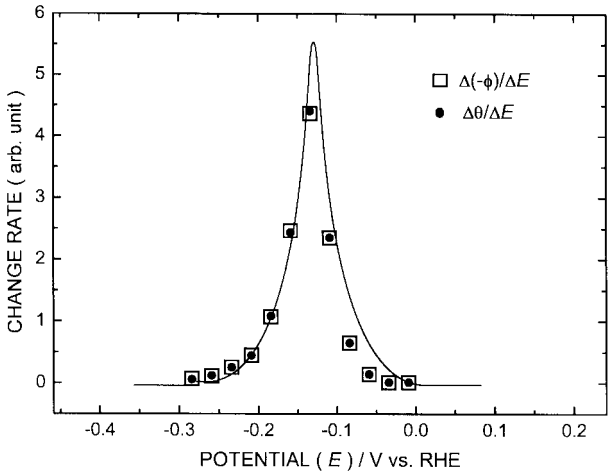

Fig. 7. The comparison of the change rates of the $\Delta(-\phi)/\Delta E$ and the $\Delta\theta/\Delta E$ for the optimum intermediate frequency (ca. 100 Hz) at the poly-Au|0.5 *M* H_2SO_4 aqueous electrolyte interface.

Figure 7 shows the comparison of the change rates of the $-\phi$ vs. E and the θ vs. E, i.e., the $\Delta(-\phi)/\Delta E$ or $d(-\phi)/dE$ and the $\Delta\theta/\Delta E$ or $d\theta/dE$, at the poly-Au|0.5 *M* H_2SO_4 aqueous electrolyte interface. The derivation of the $\Delta(-\phi)/\Delta E$ and the $\Delta\theta/\Delta E$ is based on the experimental data shown in Table 1. As expected, Table 1 and Fig. 7 show that both the $\Delta(-\phi)/\Delta E$ or $d(-\phi)/dE$ and the $\Delta\theta/\Delta E$ or $d\theta/dE$ are maximized at $\theta \approx 0.5$ and are minimized at $\theta \approx 0$ and 1. Fig. 7 also shows that a plot of the $\Delta(-\phi)/\Delta E$ or $d(-\phi)/dE$ is exactly same as that of the $\Delta\theta/\Delta E$ or $d\theta/dE$. In other words, a behavior of the phase shift ($0° \leq -\phi \leq 90°$) corresponds well to that of the fractional surface coverage ($1 \geq \theta \geq 0$). Also, it should be noted that Fig. 7 is similar to a typical shape of the change rate of the adsorption pseudocapacitance (C_ϕ) for the Langmuir adsorption conditions[27-29,32]. As previously described, it implies that the relaxation time effects of R_F and C_D, the lateral interaction effect, etc., cannot be considered or are not conflicting to analyze the adsorption process of the UPD H and/or the OPD H at the interface. In other words, the lagged phase shift ($-\phi$) described in Eq. 3 depends strongly on R_ϕ and C_ϕ, i.e., θ. For the Frumkin adsorption process, both the $\Delta(-\phi)/\Delta E$ or $d(-\phi)/dE$ and the $\Delta\theta/\Delta E$ or $d\theta/dE$ will be changed depending on the interaction parameter[21]. Also, the peak will be changed as a plateau depending on the interaction parameter. Consequently, it can be interpreted that the shape of the phase-shift profile ($-\phi$ vs. E) for the optimum intermediate frequency corresponds well to the form of the Langmuir adsorption isotherm (θ vs. E) at the interface. Both the relaxation time and lateral interaction effects on the Langmuir adsorption process are negligible at the interface.

3.3. Langmuir adsorption isotherms of the OPD H

In electrosorption, the electrode potential is introduced as an independent variable and affects the adsorption of charged species in a major way. The Volmer, the Heyrovsky, and the Tafel reactions for the cathodic HER are considered at the poly-Au|0.5 *M* H_2SO_4 aqueous electrolyte interface. However, the distinction between the Volmer, the Heyrovsky, and the Tafel reactions is not necessary and important for the Langmuir adsorption isotherm. Since, the Langmuir adsorption isotherm corresponding to the phase-shift profile for the optimum intermediate frequency is strongly dependent on the adsorption sites of the UPD H and the OPD H rather than the sequential processes for the cathodic HER.

It is assumed that the UPD H and the OPD H for the cathodic HER are an equilibrium[34]. Since, the adsorption processes of the UPD H and the OPD H are very fast compared to the mass transport processes. However, from a viewpoint of change rate with respect to time, the electrical circuit elements at the steady state are equivalent to the kinetic and thermodynamic parameters at the equilibrium. Therefore, taking into account the relaxation time effect on the ac impedance experiment and the overpotential for the cathodic HER at the interface, the state of the Langmuir adsorption isotherm corresponding to the phase-shift profile for the optimum intermediate frequency is considered as a quasi-equilibrium[35]. Also, it should be noted that both the faradaic resistance and the adsorption pseudocapacitance occur at the quasi-equilibrium[27]. It cannot exist unless charge is transferred across the interphase.

At the poly-Au electrode interface, the consideration of the Langmuir adsorption isotherm for H is more preferable to discussion in terms of an equation of the kinetics and thermodynamics for H. Since, the Langmuir adsorption isotherm can be associated more directly with the atomic mechanism of H adsorption and is experimentally determined.

The Langmuir adsorption isotherm is based on the assumptions that the surface is homogeneous and that the lateral interaction effect is negligible. The HER under the Langmuir adsorption conditions is described elsewhere[36]. Considering the application of the Langmuir adsorption isotherm to the adsorption of H on the poly-Au electrode surface, the Langmuir adsorption isotherm at the quasi-equilibrium can be expressed as follows[37]:

$$[\theta/(1 - \theta)] = KC_{H^+}[\exp(-EF/RT)] \quad (5)$$

where θ is the fractional surface coverage of the UPD H or the OPD H, K is the equilibrium constant for the UPD H or the OPD H, C_{H^+} is the H^+ concentration in the bulk electrolyte, E is the applied dc potential, F is the Faraday constant, R is the gas constant, and T is the absolute temperature. In Eq. 5, it should be noted that E is not the overpotential but the applied dc potential. The UPD H and the OPD H are a replacement reaction in which a number of water molecules are desorbed from the poly-Au electrode surface, i.e., the adsorption sites of the UPD H and the OPD H, for each H^+ adsorbed. In addition, as previously described, the fractional surface coverage (θ) of the OPD H for the cathodic HER approaches unity, i.e., $\theta \approx 1$, at high negative overpotentials.

Considering the adsorption sites on the same single-crystal faces of the poly-Pt, Ir, Au, and Rh electrode surfaces[18,19,23], the surface of the poly-Au wire can also be considered as a homogeneous surface. In other words, the imperfections in the orientation and size of the same single-crystal face substrates are not serious for the Langmuir adsorption process. Therefore, it can be assumed that the poly-Au electrode has the homo-

geneous surface. On the other hand, the oxide layer formations or the different single-crystal face substrates are serious for the Langmuir adsorption process and should be considered as an inhomogeneous surface. In this case, the Temkin or the Frumkin adsorption process should be applied to the interface[16,37].

As previously described, it is well known that the shape of the adsorption pseudocapacitance (C_ϕ vs. E) is the exact form of the Langmuir adsorption isotherm (θ vs. E)[27-29,32]. However, it is based on the numerical simulation rather than the experimental data. For the poly-Au electrode interface, it should be noted that θ by the OPD H for the cathodic HER approaches unity, i.e., $\theta \approx 1$, at high negative overpotentials as shown in Table 1. It implies that the θ vs. E for the OPD H at the poly-Au electrode interface depends strongly on the fractional surface coverage ($0 \leq \theta \leq 1$) rather than the lateral interaction effect. However, as previously described, the experimental results (Figs. 6 and 8) also show that the shape of the phase-shift profile for the optimum intermediate frequency is the exact form of the Langmuir adsorption isotherm. Consequently, it can be interpreted that the various assumptions and considerations, i.e., the simplified equivalent circuit for the optimum intermediate frequency, the relaxation time effects, the quasi-equilibrium, the homogeneous surface, the lateral interaction effect, etc., are well supplemented and compensated together for the Langmuir adsorption isotherm at the interface.

At the poly-Au|0.5 M H_2SO_4 aqueous electrolyte (pH 0.62) interface, the fitted data, i.e., the numerically calculated Langmuir adsorption isotherm using Eq. 5, are shown in Fig. 8. As expected, the Langmuir adsorption isotherm (θ vs. E) shown in Fig. 8 corresponds well to the phase-shift profile ($-\phi$ vs. E) for the optimum intermediate frequency shown in Fig. 6. From Fig. 8, it can be easily inferred that $K = 2.3\times 10^{-6}$ is applicable to the formation of H at the interface. Figures 9(a), (b), and (c) show the numerically calculated Langmuir adsorption isotherms corresponding to the three different values of $K = 2.3\times 10^{-4}$, 2.3×10^{-6}, and 2.3×10^{-8}, respectively.

The Langmuir adsorption isotherm shown in Fig. 8 is attributed to the OPD H. As expected, the Langmuir adsorption isotherm due to the UPD H has not been observed at the cathodic potential range. It is understood that the adsorption sites of the UPD H are almost masked due to a high H^+ concentration of the 0.5 M H_2SO_4 aqueous electrolyte and/or the anionic adsorption effects under the steady state conditions[5,14,15]. Also, it should be noted that the experimental data shown in Figs. 3-8 and Table 1 are observed beyond the UPD H plateau and the corresponding cathode potentials shown in Fig. 1. In other words, the Langmuir adsorption isotherm of the OPD H is located beyond that of the UPD H as shown in Fig. 14.

For the aqueous electrolyte, the standard free energy of H adsorption is given by the difference between the free energy of adsorption of H and that of a number of water molecules on the adsorption sites of the poly-Au electrode surface. Under the Langmuir adsorption conditions, the relation between the equilibrium constant for H adsorption (UPD H, OPD H) and the standard free energy (ΔG_{ads}) of H adsorption (UPD H, OPD H) is given using[37], as

$$2.3RT \log K = -\Delta G_{ads} \quad (6)$$

The definition of ΔG_{ads} is described elsewhere[16,38]. At the poly-Au|0.5 M H_2SO_4 aqueous electrolyte interface, it is readily calculated using Eq. 6 that ΔG_{ads} is 32.2 kJ/mol for $K = 2.3\times 10^{-6}$ (OPD H). As expected, in contrast to the exothermic reaction, i.e., $\Delta G_{ads} < 0$, at the UPD H region[18,19], the endothermic reaction, i.e., $\Delta G_{ads} > 0$, occurs at the OPD H region of the poly-Au electrode interface. It implies that the OPD H on the adsorption sites of the poly-Au electrode surface requires 32.2 kJ/mol to remove the appropriate number of water molecules. As shown in Fig. 8, 32.2 kJ/mol for $K = 2.3\times 10^{-6}$ (OPD H) corresponds to the applied dc potentials, i.e., ca. -0.3 to 0.05 V vs. RHE.

3.4. Transition between the Langmuir adsorption isotherms of the OPD H

Figure 10 shows the cyclic voltammogram of the steady state

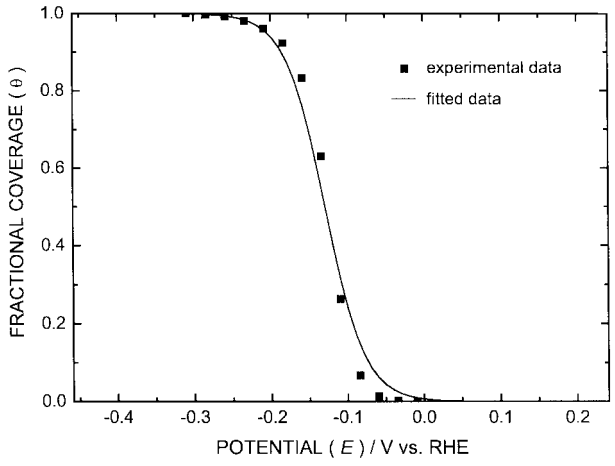

Fig. 8. The comparison of the experimental and fitted data for the Langmuir adsorption isotherms (θ vs. E) at the poly-Au|0.5 M H_2SO_4 aqueous electrolyte interface. $K = 2.3\times 10^{-6}$ (OPD H).

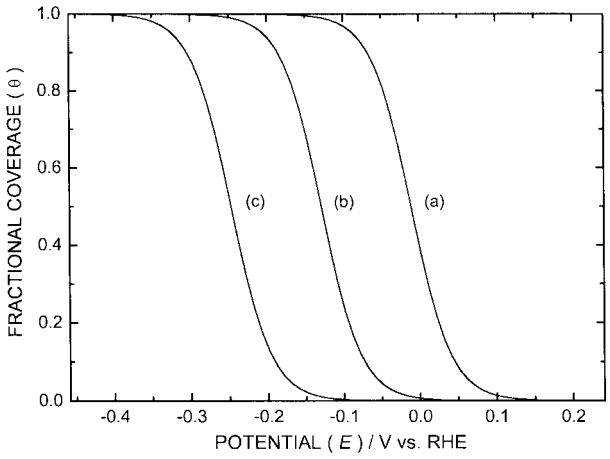

Fig. 9. The numerically calculated Langmuir adsorption isotherms (θ vs. E) at the poly-Au|0.5 M H_2SO_4 aqueous electrolyte interface. (a) $K = 2.3\times 10^{-4}$, (b) $K = 2.3\times 10^{-6}$, and (c) $K = 2.3\times 10^{-8}$.

at the poly-Rh|0.5 *M* H_2SO_4 aqueous electrolyte interface. The UPD H peak occurs at ca. 0.039 V vs. RHE. The Rh electrode interface has the closest resemblance to the Pt electrode interface except for the overall cathodic shift by about 0.3 V for the onset of the adsorption and desorption of oxygen. The feature of the cyclic voltammogram shown in Fig. 10 is described elsewhere[12,39,40]. However, as previously described, the UPD H peak and the corresponding cathode potential are necessary and useful to verify the Langmuir adsorption isotherms of the UPD H and the OPD H for the cathodic HER at the poly-Rh electrode interface.

Figure 11 shows the comparison of the phase-shift curves (-ϕ vs. *f*) for the different cathode potentials at the poly-Rh|0.5 *M* H_2SO_4 aqueous electrolyte interface. As shown in Fig. 5, Fig. 11 also shows that the lagged phase shifts and related phase-shift curves are markedly characterized at the intermediate frequencies.

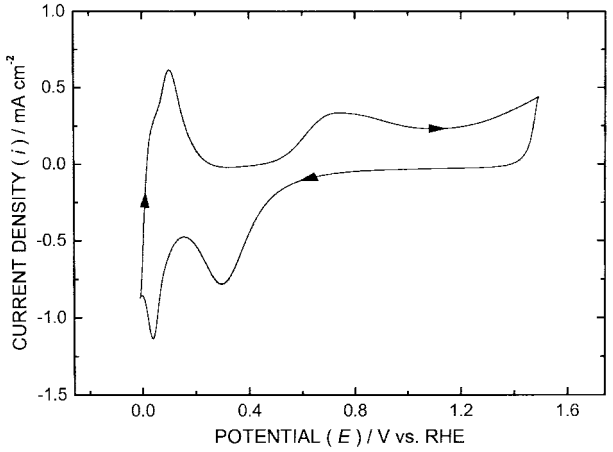

Fig. 10. The typical cyclic voltammogram at the poly-Rh|0.5 *M* H_2SO_4 aqueous electrolyte interface. Estimated surface area: ~1.17 cm^2. Scan potential: -0.009 to 1.491 V vs. RHE. Scan rate: 200 mV/s. 20th scan.

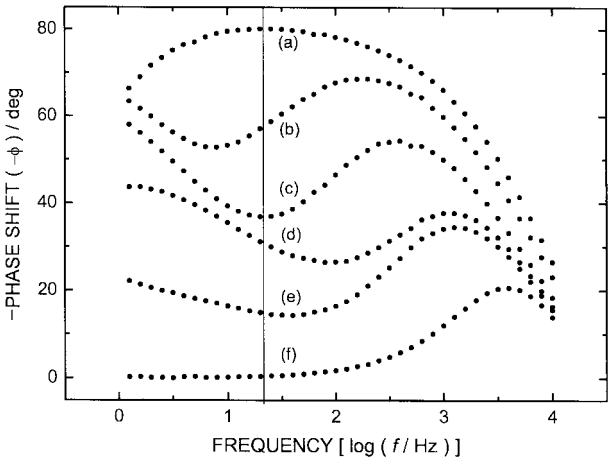

Fig. 11. The comparison of the phase-shift curves at the poly-Rh|0.5 *M* H_2SO_4 aqueous electrolyte interface. Vertical solid line: ca. 25 Hz. Single sine wave. Scan frequency: 10^4 to 1 Hz. ac amplitude: 5 mV. dc potential: (a) 0.241 V, (b) 0.116 V, (c) 0.066 V, (d) -0.009 V, (e) -0.034 V, and (f) -0.184 V vs. RHE.

Figures 12 and 13 show the phase-shift profile (-ϕ vs. *E*) for the optimum intermediate frequency (ca. 25 Hz) and the corresponding Langmuir adsorption isotherm (θ vs. *E*) at the poly-Rh|0.5 *M* H_2SO_4 aqueous electrolyte interface, respectively. As expected, Figs. 12 and 13 also show that the -ϕ vs. *E* corresponds well to the θ vs. *E* at the interface. Figs. 12 and 13 are obtained through the previously described procedures. In Figs. 12 and 13, both the regions (a) and (b) correspond to the OPD H region. It should be noted that the Langmuir adsorption isotherms of the OPD H shown in Figs. 13(a) and (b) are located beyond the UPD H peak (ca. 0.039 V vs. RHE) on the cyclic voltammogram shown in Fig. 10 and the corresponding cathode potential.

Figures 14 (c) and (d) show the numerically calculated Langmuir adsorption isotherms (θ vs. *E*) corresponding to the two different values of *K* shown in Figs. 13 (a) and (b), respectively. Figs. 14 (c) and (d) also show that the transition region (ca. 0.087 to -0.002 V vs. RHE) shown in Figs. 13 (a)

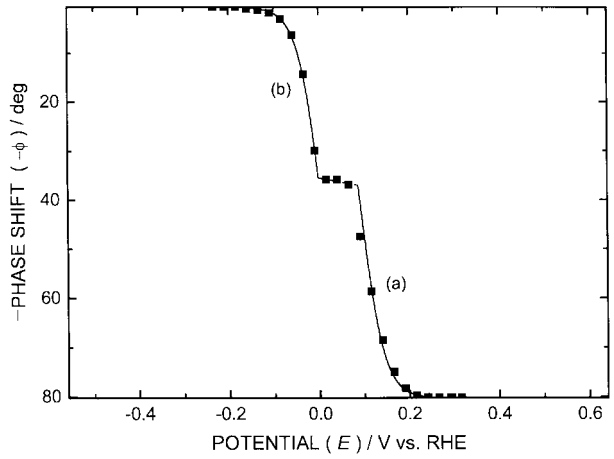

Fig. 12. The phase-shift profile (-ϕ vs. *E*) for the optimum intermediate frequency (ca. 25 Hz) at the poly-Rh|0.5 *M* H_2SO_4 aqueous electrolyte interface. (a) OPD H and (b) OPD H regions.

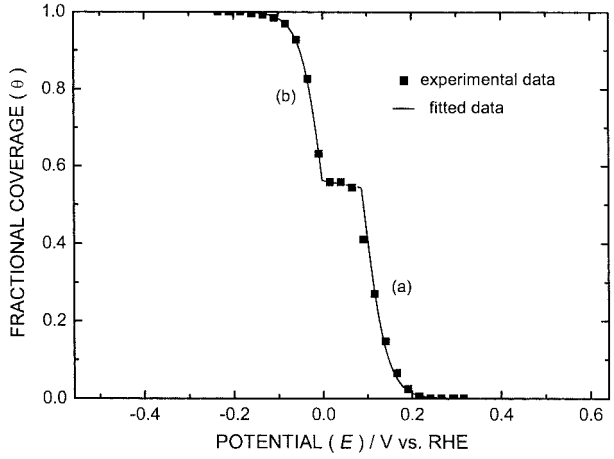

Fig. 13. The comparison of the experimental and fitted data for the Langmuir adsorption isotherm (θ vs. *E*) at the poly-Rh|0.5 *M* H_2SO_4 aqueous electrolyte interface. (a) $K = 1.2 \times 10^{-2}$ (OPD H) and (b) $K = 4.1 \times 10^{-4}$ (OPD H).

and (b) is related to the overlapped region between the Langmuir adsorption isotherms of the OPD H. It implies that the two processes of the OPD H for the cathodic HER at the poly-Rh electrode interface proceed independently of each other. In other words, the two processes of the OPD H are the independent processes depending on the adsorption sites of the OPD H rather than the sequential processes for the cathodic HER. However, as expected, the value of K of the UPD H is much (~10^3-10^6 times) greater than that of the OPD H[18,19,23]. It implies that only the OPD H can contribute to the cathodic HER.

Under the Langmuir adsorption conditions[37], the transition region implies that the equilibrium constant for H adsorption and the standard free energy (ΔG_{ads}) of H adsorption shift depending on the applied dc potential, i.e., the cathode potential. In other words, the poly-Rh electrode surface has the two different adsorption sites of the OPD H corresponding to the two different values of K or ΔG_{ads}. Figs. 12 and 13 show that K transits from 1.2×10^{-2} (OPD H) to 4.1×10^{-4} (OPD H) depending on E and vice versa. Similarly, Figs. 12, 13, and Eq. 6 imply that ΔG_{ads} transits from 11.0 kJ/mol (OPD H) to 19.3 kJ/mol (OPD H) depending on E and vice versa. It also implies that the endothermic reaction, i.e., $\Delta G_{ads} > 0$, occurs at the OPD H region of the poly-Rh | 0.5 M H_2SO_4 aqueous electrolyte interface. However, it can be interpreted that the two different adsorption sites of the OPD H on the poly-Rh electrode surface act as two distinguishable electro-adsorbed H species. At present, it is unclear whether the two different Langmuir adsorption isotherms of the OPD H are attributed to the preparation, e.g., cutting, polishing, etc., or the nature, e.g., purity, oxide layer, etc., of the poly-Rh electrode surface. Finally, Table 2 shows that the endothermic reaction occurs at the adsorption sites of the OPD H on the noble and transition metal (Au, Rh, Pt, Ir, Pd, Ni) electrode surfaces[17-21].

Table 2. The comparison of the equilibrium constant (K) and standard free energy (ΔG_{ads}) of the OPD H at the noble and transition metal (Au, Rh, Pt, Ir, Pd, Ni)|aqueous electrolyte interfaces

Electrode | Electrolyte	K	ΔG_{ads} (kJ/mol)	Reference
poly-Au | 0.5 M H_2SO_4 [a]	2.3×10^{-6}	32.2	-
poly-Rh | 0.5 M H_2SO_4 [a]	4.1×10^{-4} 1.2×10^{-2}	19.3 11.0	-
Pt(100) | 0.5 M H_2SO_4 [a,*]	1.5×10^{-4}	21.8	19
poly-Pt | 0.5 M H_2SO_4 [a]	2.1×10^{-4}	21.0	20
poly-Ir | 0.1 M H_2SO_4 [a]	2.0×10^{-4}	21.1	18
poly-Pd | 0.1 M H_2SO_4 [b]	5.0×10^{-7} 1.0×10^{-5}	35.9 28.5	17
poly-Ni | 0.05 M KOH [b]	5.9×10^{-6} 0.13	29.8 5.1	21
poly-Ni | 1 M NaOH	4.2×10^{-6} 0.1	30.7 5.7	3,7

[a]Langmuir adsorption process.
*Commercially prepared single-crystal disc.
[b]Frumkin adsorption process.

3.5. Comment on the existing thermodynamic results

The comparison of the obtained experimental data and the existing thermodynamic results is important and necessary to confirm the validity and significance of the phase-shift method for the Langmuir adsorption isotherms of the OPD H. The validity and significance of the phase-shift method for the Langmuir or the Frumkin adsorption isotherms of the OPD H at the poly-Pt and Ni | aqueous electrolyte interfaces are described elsewhere[20,21].

The thermodynamic results for the UPD H on the poly-Rh electrode surface have been intensively studied by Jerkiewicz *et al.*[1,2]. In contrast to the UPD H, it seems to be that the equilibrium constant and standard free energy of the OPD H at the poly-Rh | 0.5 M H_2SO_4 aqueous electrolyte interface have not been reported elsewhere. However, it is understood that the obtained experimental data, i.e., ΔG_{ads} of the OPD H: 11.0 kJ/mol for $K = 1.2\times 10^{-2}$ or 19.3 kJ/mol for $K = 4.1\times 10^{-4}$, shown in Fig. 13 are well complementary to the existing thermodynamic results, i.e., ΔG_{ads} of the UPD H: -17 to -8 kJ/mol, shown in Refs. 1 and 2. As expected, in contrast to the OPD H region, the exothermic reaction, i.e., $\Delta G_{ads} < 0$, occurs at the UPD H region. It implies that the UPD H on the adsorption sites of the poly-Rh electrode surface is the spontaneous adsorption process. From the existing thermodynamic results, it is readily calculated using Eq. 6 that K is 9.6×10^2 for ΔG_{ads} = -17 kJ/mol (UPD H) and is 25.3 for ΔG_{ads} = -8 kJ/mol (UPD H).

Figures 14(a), (b), (c), and (d) show the Langmuir adsorption isotherms (θ vs. E) corresponding to the existing thermodynamic results, i.e., $K = 9.6\times 10^2$ for ΔG_{ads} = -17 kJ/mol (UPD H) and K = 25.3 for ΔG_{ads} = -8 kJ/mol (UPD H)[1,2], and the obtained experimental data, i.e., $K = 1.2\times 10^{-2}$ for ΔG_{ads} = 11.0 kJ/mol (OPD H) and $K = 4.1\times 10^{-4}$ for ΔG_{ads} = 19.3 kJ/mol (OPD H), respectively. In contrast to the nebulous thermodynamic distinction between the UPD H and the OPD H[14,15], the Langmuir adsorption distinction between the UPD H and the OPD H is plotted clearly as shown in Fig. 14. However,

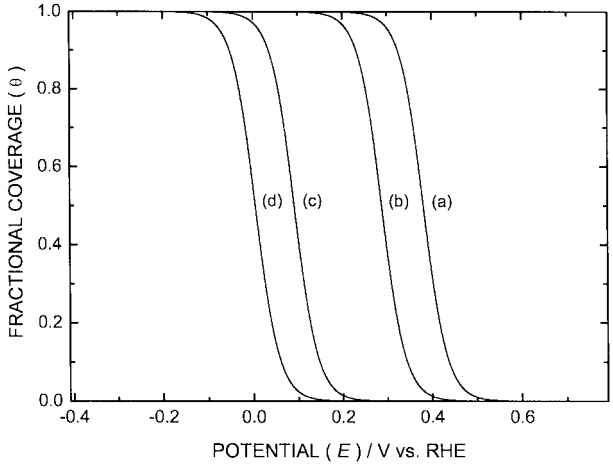

Fig. 14. The comparison of the numerically calculated Langmuir adsorption isotherms (θ vs. E) at the poly-Rh | 0.5 M H_2SO_4 aqueous electrolyte interface. (a) $K = 9.6\times 10^2$ (UPD H) (b) K = 25.3 (UPD H)[7,8], (c) $K = 1.2\times 10^{-2}$ (OPD H), and (d) $K = 4.1\times 10^{-4}$ (OPD H).

it should be noted that the Langmuir adsorption isotherms of the OPD H shown in Figs. 13(a) and (b) are located beyond the region of the UPD H peak on the cyclic voltammogram shown in Fig. 10. In Fig. 14, as expected, *K* of the UPD H is about 10^3-10^6 times greater than that of the OPD H. It implies that the experimental data presented using the phase-shift method and related discussions are reasonable and valid at the interfaces.

Figure 14 also shows that the UPD H and the OPD H are the independent processes depending on the H adsorption sites on the poly-Rh electrode surface rather than the sequential processes for the cathodic HER. Considering the independent processes of the UPD H and OPD H, i.e., the two different adsorption sites of the UPD H and the OPD H, the superposition or the extension between the Langmuir adsorption isotherms of the UPD H and the OPD H cannot be occurred at the cathodic potential range. Therefore, as expected, the overlapped region between the Langmuir adsorption isotherms of the UPD H and the OPD H must be occurred as shown in Fig. 14. Also, it can be explained that θ of the UPD H has reached unity already at the onset of the OPD H. Of course, as previously described, there is neither the superposition nor the extension between the Langmuir adsorption isotherms of the UPD H and the OPD H at the cathodic potential range. It also has been confirmed at the Pt and Ir electrode interfaces[18-20]. Consequently, it can be interpreted that the Langmuir adsorption isotherms shown in Figs. 8 and 13 are attributed to the OPD H for the cathodic HER. The experimental data presented using the phase-shift method for the OPD H are well complementary to the existing thermodynamic results for the UPD H.

Finally, the relationship between the phase-shift profile (-ϕ vs. *E*) for the optimum intermediate frequency and the Langmuir adsorption isotherm (θ vs. *E*) of the OPD H for the cathodic HER should be represented theoretically or numerically at the interfaces. At present, the effects of relaxation times and various adsorptions on the adsorption sites of the UPD H and the OPD H have not been combined into a single equation for the relationship. Therefore, it seems to be difficult or needs a lot of times to make the relationship basis on theoretical derivation or numerical calculation.

4. Conclusions

The phase-shift method for the Langmuir adsorption isotherm of the OPD H for the cathodic HER is proposed. The simplified equivalent circuit for the optimum intermediate frequency and the corresponding phase-shift equation are well fitted to the poly-Au and Rh|0.5 *M* H_2SO_4 aqueous electrolyte interfaces regardless of H_2 evolution. The behavior of the phase shift ($0^o \leq -\phi \leq 90^o$) for the optimum intermediate frequency corresponds well to that of the fractional surface coverage ($1 \geq \theta \geq 0$) at the interfaces. The phase-shift profile (-ϕ vs. *E*) for the optimum intermediate frequency, i.e., the phase-shift method, can be effectively used as a new electrochemical method to determine the Langmuir adsorption isotherm (θ vs. *E*) of the OPD H for the cathodic HER at the interfaces. At the poly-Au|0.5 *M* H_2SO_4 aqueous electrolyte interface, the equilibrium constant (*K*) and the standard free energy (ΔG_{ads}) of the OPD H are 2.3×10^{-6} and 32.2 kJ/mol, respectively. At the poly-Rh|0.5 *M* H_2SO_4 aqueous electrolyte interface, *K* and ΔG_{ads} of the OPD H are 4.1×10^{-4} or 1.2×10^{-2} and 19.3 or 11.0 kJ/mol depending on *E*, respectively. In contrast to the poly-Au electrode interface, the two different Langmuir adsorption isotherms of the OPD H are observed at the poly-Rh electrode interface. The two different Langmuir adsorption isotherms of the OPD H correspond to the two different adsorption sites of the OPD H on the poly-Rh electrode surface.

Acknowledgements

The authors thank Professor G. Jerkiewicz (Department of Chemistry, Queens University, Kingston, Canada) for his valuable suggestions and encouragement on the phase-shift method.

A part of this paper has been appeared in Journal of the Electrochemical Society (Vol. 150, No. 4, E207-217). It is reproduced by permission of The Electrochemical Society, Inc.

References

1. A. Zolfaghari, F. Villiard, M. Chayer, and G. Jerkiewicz, *J. Alloys Compounds*, **253-4**, 481 (1997).
2. G. Jerkiewicz, *Prog. Surf. Sci*., **57**, 137 (1998).
3. A. Lasia and A. Rami, *J. Electroanal. Chem*., **294**, 123 (1990).
4. A. Lasia, in *Electrochemistry and Materials Science of Cathodic Hydrogen Absorption and Adsorption*, B. E. Conway and G. Jerkiewicz, Editors, PV 94-21, pp. 261-282, The Electrochemical Society, Pennington, NJ (1995).
5. M. W. Breiter, G. Staikov, and W. J. Lorenz, in *Electrochemistry and Materials Science of Cathodic Hydrogen Absorption and Adsorption*, B. E. Conway and G. Jerkiewicz, Editors, PV 94-21, pp. 152-166, The Electrochemical Society, Pennington, NJ (1995).
6. D. A. Harrington and B. E. Conway, *Electrochim. Acta*, **32**, 1703 (1987).
7. J. Barber, S. Morin S, and B. E. Conway, *J. Electroanal. Chem*., **446**, 125 (1998).
8. G. Jerkiewicz and A. Zolfaghari, *J. Phys. Chem*., **100**, 8454 (1996).
9. A. Zolfaghari, M. Chayer, and G. Jerkiewicz, *J. Electrochem. Soc*., **144**, 3034 (1997).
10. S. Morin, H. Dumont, and B. E. Conway, *J. Electroanal. Chem*., **412**, 39 (1996).
11. A. Zolfaghari and G. Jerkiewicz, *J. Electroanal. Chem*., **467**, 177 (1999).
12. G. Jerkiewicz and A. Zolfaghari, in *Electrochemistry and Materials Science of Cathodic Hydrogen Absorption and Adsorption*, B. E. Conway and G. Jerkiewicz, Editors, PV 94-21, pp. 31-43, The Electrochemical Society, Pennington, NJ (1995).
13. B. E. Conway, in *Interfacial Electrochemistry*, A. Wieckowski, Editor, pp. 131-150, Marcel Dekker, New York (1999).
14. B. E. Conway and G. Jerkiewicz, *Electrochim. Acta*, **45**, 4075 (2000).
15. B. E. Conway and G. Jerkiewicz, in *Hydrogen at Surfaces and Interfaces*, G. Jerkiewicz, J. M. Feliu, and B. N. Popov, Editors, PV 2000-16, pp. 1-11, The Electrochemical Society, Pennington, NJ (2000).
16. E. Gileadi, in *Electrosorption*, E. Gileadi, Editor, pp. 1-18, Plenum

Press, New York (1967).
17. J. H. Chun and K. H. Ra, *J. Electrochem. Soc*., **145**, 3794 (1998).
18. J. H. Chun and K. H. Ra, in *Hydrogen at Surfaces and Interfaces*, G. Jerkiewicz, J. M. Feliu, and B. N. Popov, Editors, PV 2000-16, pp. 159-173, The Electrochemical Society, Pennington, NJ (2000).
19. J. H. Chun, K. H. Ra, and N. Y. Kim, *Int. J. Hydrogen Energy*, **26**, 941 (2001).
20. J. H. Chun, S. K. Jeon, and J. H. Lee, *J. Korean Electrochem. Soc*., **5**, 131 (2002).
21. J. H. Chun, K. H. Ra, and N. Y. Kim, *J. Electrochem. Soc*., **149**, E325 (2002).
22. J. H. Chun and S. K. Jeon, *J. Korean Electrochem. Soc*., **4**, 118 (2001).
23. J. H. Chun, K. H. Ra, and N. Y. Kim, *J. Electrochem. Soc*., **150**, E207 (2003).
24. J. H. Chun and S. K. Jeon, *Int. J. Hydrogen Energy*, **28**, in press (2003).
25. E. Gileadi, E. Kirowa-Eisner, and J. Penciner, *Interfacial Electrochemistry*, pp. 6-13, 72-73, Addison-Wesley Pub. Co., Reading, MA (1975).
26. D. M. Macarthur, in *Characterization of Solid Surfaces*, P. F. Kane and G. B. Larrabee, Editors, pp. 181-201, Plenum Press, New York (1978).
27. E. Gileadi, E. Kirowa-Eisner, and J. Penciner, *Interfacial Electrochemistry*, pp. 86-93, Addison-Wesley Pub. Co., Reading, MA (1975).
28. E. Gileadi, *Electrode Kinetics*, pp. 293-303, VCH, New York (1993).
29. S. Sarangapani, B. V. Tilak, and C. P. Chen, *J. Electrochem. Soc*., **143**, 3791 (1996).
30. R. D. Armstrong and M. Henderson, *J. Electroanal. Chem*., **39**, 81 (1972).
31. J. G. Holbrook, *Laplace Transforms for Electronic Engineers*, pp. 141-146, Macmillan Co., New York (1959).
32. E. Gileadi and B. E. Conway, in *Modern Aspects of Electrochemistry*, JOM. Bockris and B. E. Conway, Editors, Vol. 3, Chap. 5, Butterworth, Washington, DC (1964).
33. J. H. Chun, K. H. Mun, and C. D. Cho, *J. Korean Electrochem. Soc*., **3**, 25 (2000).
34. A. K. N. Reddy, in *Electrosorption*, E. Gileadi, Editor, pp. 53-71, Plenum Press, New York (1967).
35. E. Gileadi, E. Kirowa-Eisner, and J. Penciner, *Interfacial Electrochemistry*, pp. 78-79, Addison-Wesley Pub. Co., Reading, MA (1975).
36. A. J. Apple, in *Comprehensive Treatise of Electrochemistry*, B. E. Conway et al., Editors, Vol. 7, pp. 218-228, Plenum Press, New York (1983).
37. E. Gileadi, *Electrode Kinetics*, pp. 261-271, VCH, New York (1993).
38. E. Gileadi, *Electrode Kinetics*, pp. 307-318, VCH, New York (1993).
39. D. T. Sawyer and J. L. Roberts Jr., *Experimental Electrochemistry for Chemists*, p. 67, Wiley, New York (1974).
40. M. Enyo, in *Comprehensive Treatise of Electrochemistry*, B. E. Conway et al., Editors, Vol. 7, pp. 241-300, Plenum Press, New York (1983).